Pure & Appl. Chem., Vol. 67, No. 6, pp. 1003–1010, 1995.
Printed in Great Britain.

Thermodynamics and transport processes in reactor fuel

Donald R. Olander

Department of Nuclear Engineering, University of California, Berkeley, CA 94720

Abstract: Chemical thermodynamics and transport processes are inextricably linked in light-water reactor fuel rods. Two regimes can be identified, separated by their temperatures. During *normal operation,* the temperature at the center of the UO_2 pellet usually does not exceed 1000°C, and most of the important chemistry takes place at the periphery, which is separated from the Zircaloy cladding by a thin(tens of microns) gas-filled gap. The temperatures here are typically 350-600°C . In a serious accident resulting in loss of cooling water circulating in the reactor's primary circuit, *severe fuel damage* may occur. Conditions in this regime encompass temperatures from ~1000 to 3000°C, the state of water is steam rather than liquid, and the system total pressure may be as low as 1 atm. This paper reviews the important chemistry-transport phenomena that occur in the normal-operation and severe-fuel-damage regimes.

I Normal Operation

Normal operation includes two sub regimes: operation with *intact* fuel rods and operation with *defective* rods.

Intact Fuel Rods

The chemistry in a fuel rod with flaw-free cladding is rather benign, and exhibits two main features. First, fission of uranium in UO_2 is an oxidizing process. When an atom of uranium disappears by fission, two atoms of oxygen are left without the strong chemical binding afforded by the departed U^{4+} ion. In its place are two fission product atoms. Tetravalent fission products such as Zr and Mo rebind the freed O atoms. However, the bulk of the fission products either bind fewer than two oxygen atom(e.g., rare earths, barium, cesium) or none at all(e.g., xenon, noble metals, iodine). When the oxygen-binding capacities of the spectrum of elements produced by fission are averaged over their yields, a net excess of oxygen develops. However, this excess is readily absorbed by the cladding in the form of a thin layer of ZrO_2 in the inner wall. This inner oxide scale is not large enough to compromise the integrity of the cladding.

The second feature of the chemistry of intact fuel rods involves the volatile fission products that are released from the fuel in small quantities. The fuel swells during normal operation because of fission product accumulation, and when it contacts the cladding, tensile stresses are set up in the latter. The combination of stress and the presence of chemically-reactive species such as iodine on an alloy such as Zircaloy can lead to cladding failure by stress-corrosion cracking. This phenomenon is called pellet-cladding interaction(PCI) and the flaws it produces in the cladding are usually small through-wall holes or narrow cracks.

Defective Fuel Rods

On the rare occasions that the cladding is perforated by a small hole, communication between the main coolant and the gas volume inside the rod is established. Small flaws in the cladding, which are usually caused by debris fretting, the PCI process described above, or manufacturing defects, are detected by an increase in the radioactivity of the coolant due to release of volatile fission products xenon and iodine from the fuel rod interior. The presence of such defects is generally not cause for shutting down the reactor. Rather, the concern is that the chemical processes that follow entry of steam into the gap can lead to more serious degradation of the cladding, often in the form of long axial cracks. This type of degradation allows significant quantities of fuel to be swept onto the coolant stream, and necessitates reactor shutdown to remove the assembly containing the defective rod. This type of failure does not compromise the safety of the system; rather, it is the economic penalty attendant to loss of electrical power production and the impediment to routine maintenance of components of the primary coolant circuit by high levels of

background radiation that are of principal concern.

When a small defect penetrates the cladding, coolant rapidly flows into the rod free volume. As liquid water enters the rod via the defect, it flashes to steam because the temperature in the rod interior is higher than the saturation temperature at system pressure. The gas volume consists chiefly of a plenum above the fuel stack and the gap between the fuel and the cladding. Even if the fuel and cladding are in contact, roughness of the two surfaces and cracks in the fuel provide an effective gap thickness on the order of 20 μm(1). The initial pressure equilibration process is very fast(seconds to minutes) compared to subsequent chemical and transport processes. These are sketched in Fig. 1.

In the gap, steam reacts with the inner wall of the cladding to produce hydrogen and additional oxide scale on the metal:

$$Zr + 2H_2O \rightarrow ZrO_2 + 2H_2 \quad (1)$$

Molecular diffusion limits the supply of steam to locations in the gap far removed from the steam source at the primary defect. Consequently, the gas becomes steam-starved in these regions. Although the standard free energy change of reaction(1) is large and the reaction free energy is negative even for large H_2/H_2O ratios, the rate of oxidation becomes slower as the gas is depleted of steam. At hydrogen-to-steam ratios on the order of 10^4 - 10^5, oxidation is insufficient to maintain a protective oxide scale on the metal. Intact oxide layers on the inner cladding surface prevent entry of hydrogen into the metal because of the very low solubility of H_2 in ZrO_2(2). In steam-starved gases, H_2 can penetrate defects in the oxide layer and cause hydriding of the metal:

$$Zr + H_2 \rightarrow ZrH_2 \text{ (}\delta\text{-hydride)} \quad (2)$$

When H_2 contacts the metal, the hydride rapidly forms because the equilibrium pressure of H_2 over the two-phase Zr/δ-hydride is far lower than the 7 - 15 MPa pressure of H_2 in the steam-starved gas. The hydride that forms has a lower density than the metal and consequently produces high stresses in the cladding in this region. It is this stress coupled with the brittleness of the hydride phase that causes extensive cracking over large lengths of the cladding.

Reaction(1) is not the only source of hydrogen inside the gap. Although even pure steam cannot thermodynamically oxidize UO_2 to UO_{2+x}, the gas in the gap is subjected to radiolysis by the intense flux of fission fragments recoiling from the fuel surface. Radiolytic decomposition of water vapor produces H_2 and a variety of oxidizing radiolysis products(ORP), chief of which are H_2O_2 and the free radicals HO_2, and OH. Steam decomposition by radiation can be symbolically expressed by:

$$H_2O \Rightarrow H_2 + ORP \quad (3)$$

The oxidizing power of the ORP far exceeds that of water vapor, and even in the presence of excess H_2, these species can cause fuel oxidation:

$$UO_2 + ORP \rightarrow UO_{2+x} + H_2 \quad (4)$$

Not only does fuel oxidation produce additional H_2 to supplement that provided by reaction(1), but the oxidized fuel has several undesirable properties; it has a lower thermal conductivity than UO_2, which causes the fuel temperature to rise. Higher temperatures, abetted by the higher mobility of impurity atoms in the defected structure of the hyperstoichiometric oxide, enhances release of fission gas from the fuel. This gas enters the gap and diffuses towards the primary defect, whence it exits and adds to the radioactivity of the coolant.

When the secondary hydride fracture in the cladding becomes large enough, coolant directly contacts the exposed fuel. The water contains dissolved O_2(at the sub ppm level) sufficient to oxidize UO_2 to UO_3, crystals of which have been observed on fuel at locations contacting the coolant. The UO_3 phase is easily eroded by the flowing water, sweeping pieces of irradiated fuel into the primary circuit.

Analysis of this complex process to provide a computational tool of sufficient accuracy to permit prediction of the course of rod degradation following observation of a primary defect is a daunting challenge. It requires combining the thermodynamics of the relevant reactions with the kinetics of gas-phase diffusion in the gap, the rates of the gas-solid reactions, the effect of gas radiolysis, and the mechanics of hydride crack formation and propagation in the stressed cladding. Such a computational tool is essential for prediction of

fuel performance in the extended-burnup fuel cycles contemplated for future reactor operation.

II Severe Fuel Damage(SFD)

The type of materials chemistry phenomena that occur during a severe reactor accident are basically the same as those that occur during normal operation of a defective fuel rod, but take place at much faster rates because the temperature is higher. Oxidation and hydriding of the cladding and fission product release are still major contributors to the event. However, radiolytic effects are absent because no fission occurs. In addition, direct chemical interaction between the fuel and cladding is important at high temperature.

Cladding Oxidation

Cladding oxidation by steam is important in SFD because of the heat released and the hydrogen produced. When the steam is plentiful, the cladding becomes fully oxidized to ZrO_2 before the melting point of the metal is reached. However, if the majority of the water has escaped the core and if the emergency core cooling system is not operating, steam blankets the fuel rods. Under these circumstances, the large mass of zirconium in the core(~25 tons for a 1000 MWe reactor) can produce so much hydrogen by reaction (1) that the gas phase becomes severely depleted in water vapor. In this event, the cladding does not completely oxidize, and the ZrO_2 scale dissolves in the remaining metal before the latter melts. The large accident-modeling codes written for the purpose of analyzing severe accidents describe zircaloy oxidation by parabolic corrosion rate theory(3-5). This model assumes that oxidation takes place in an environment of unlimited steam, and so fails to account for the details of the morphological changes that occur in steam-starved corrosion. As will be seen, the presence or absence of a ZrO_2 scale on the cladding has profound effects on the uptake of hydrogen by the metal and on the course of the fuel dissolution process that begins when the metal melts.

Because of poor heat removal when rapidly-flowing liquid water is replaced by slowly-rising steam produced by vaporization of the water pool at the bottom of the core, the temperature of the fuel rod rises in response to the energy deposition in the fuel and cladding by the β and γ radiation from the decay of fission products in the fuel. When the temperature reaches ~1000°C, decay heating is supplemented by oxidative heating driven by the heat release of reaction(1).

Analysis of the oxidation process involves coupling of axial gas transport in the hydrogen-steam mixture with radial transport of oxygen into the cladding by solid-state diffusion. The gas, oxide, and metal phases are coupled by the assumption of thermodynamic equilibrium at the phase boundaries.

The fuel rod is divided axially into nodes of equal height ΔX, each of which communicates with its lower neighbor by a convective term representing the velocity of the rising gas. The steam conservation equation for node i is given by:

$$\frac{dy}{dt} = \frac{v}{\Delta X}(y' - y) - \frac{2\pi a}{S_g C_g} j \tag{5}$$

where y' and y are the mole fractions of water vapor in the gas entering and leaving a node, respectively, C_g is the total molar gas concentration, v is the velocity of the gas, a is the fuel pellet radius, S_g is the cross-sectional area of coolant channel associated with each fuel rod, and j is the flux of water into the cladding. This flux is determined by the gas-phase mass transfer resistance in the steam-hydrogen mixture in series with solid state diffusion of oxygen in the oxide scale, which leads to the radial oxygen flux equation:

$$j = k_g C_g (y - y_s) = D_O^{ox} \rho_{ox} (C_s - C_a)/\delta \tag{6}$$

where k_g is the gas-phase mass transfer coefficient, and y and y_S are the steam mole fractions in the bulk gas and in the gas at the surface, respectively. D_O^{ox} is the diffusion coefficient of oxygen in ZrO_2, ρ_{OX} is the molar concentration of Zr in ZrO_2, and C_S and C_a are the O/Zr ratios of the oxide at the gas-scale interface and at the scale-metal interface, respectively. The latter is fixed by the Zr/O phase diagram. Equation(6) is coupled to the thermodynamic condition that relates the surface O/Zr ratio to the water vapor mole fraction in the gas phase. This relation, $y_S=F(C_S,T)$ provides an additional equation that enables the surface concentrations to be eliminated in terms of the bulk gas concentration and the oxide scale thickness. The function $F(C_S,T)$ is available(6), and shows a very steep rise as the oxide approaches stoichiometry($C_S = 2$). This behavior simplifies evaluation of the surface concentrations; either $C_S = 2$ and $y_S>0$ or $C_S < 2$ and $y_S = 0$. The latter state is referred to as steam starvation, and the oxygen absorption rate is gas-phase-mass transfer controlled.

In addition, oxygen transport from the fuel to the cladding occurs by the gas-phase H_2O/H_2 transport mechanism, leading to reduction of the fuel from UO_2 to UO_{2-x} and corresponding internal oxidation of the cladding. This effect is small compared to external oxidation.

Oxygen transport in the metal portion of the cladding is driven by the concentration distributions shown in Fig. 2 and is described by the moving-boundary diffusion equation:

$$\frac{\partial C}{\partial t} = D_O^M \frac{\partial^2 C}{\partial z^2} + G \frac{d\delta}{dt} \frac{\partial C}{\partial z} \tag{7}$$

where C is the O/Zr ratio in the metal, D_O^M is the diffusion coefficient of oxygen in Zircaloy, G^{-1} is the Pilling-Bedworth ratio of ZrO_2, and δ is the thickness of the oxide layer.

Neglecting the oxygen uptake due to reduction of the fuel, Eqs(5) - (7) can be solved numerically by the integral diffusion method described in Ref. 7.

The method is applied to the conditions of the tests described in Ref. 8, which represent a generic accident scenario in a PWR. The fuel rod consists of 1 cm diameter fuel pellets with 1 mm thick cladding. The upward gas velocity is 1 cm/s. The total gas pressure is 15 MPa and the temperature is assumed to rise at a rate of 1 K/s independent of elevation in a 2 m length of core above the location where the temperature is 1000°C. The gas phase mass transfer coefficient is taken to be 0.2 cm/s and the solid state diffusion coefficients of oxygen in the metal and the oxide are taken from Ref. 7. The initial total oxygen content of the cladding is partitioned into 80% in the oxide scale and 20% in the metal, the latter corresponding to an as-fabricated O/Zr ratio of 0.015 and the former to a pre-accident scale thickness of 50 μm.

Figure 3 shows the calculated bulk gas steam mole fractions at three heights along the fuel rod as functions of time. For t<200 - 300 s, the gas phase remains essentially pure steam because the steam removal rate by oxidation is small at temperature below about 1300°C. At higher temperatures, the oxygen diffusion coefficients become large enough for corrosion to become a significant sink for water in the bulk gas. The steam mole fractions drop rapidly with time and in less than a few hundred seconds, reach the water vapor concentration in equilibrium with fully-reduced zirconia(bottom curve in Fig. 3). The horizontal dashed line represents the steam concentration in the gas at which the surface of the cladding becomes steam starved(i.e., $y_S = 0$).

Figure 4 shows the time dependence of the scale thickness relative to the total cladding thickness at three elevations. The oxide scale disappears by dissolution into the substrate metal at times between 300 and 500 s. This phenomenon cannot be predicted by the parabolic scaling theory used in current accident analysis codes(3-5).

Figure 5 shows the states of the cladding on a time-elevation projection. The dashed curve represents the locus of points at which steam starvation occurs. Time-location combinations in regions inside the arrows are steam-starved. The times at which the oxide scale completely dissolves in the metal is shown as the solid line in Fig. 5. At points to the right of this curve, the cladding is Zircaloy with a spatially-uniform distribution of dissolved oxygen. No further oxidation of the cladding or change in its physical state occurs unless additional steam enters the axial node.

The detailed morphological state of the cladding shown in Fig. 5 is important because it determines: i) the heat released by the oxidation process; ii) hydrogen dissolution in the cladding; and iii) the capacity of the metal to dissolve fuel when the cladding melts at ~2000°C.

Oxidative Heating

All severe accident codes(3-5) compute the heat release from the standard enthalpy change of reaction(1). However, during a substantial portion of the accident, the corrosion product is not the stoichiometric oxide. In steam-starved regions, the principal final state is oxygen dissolved in the metal, and the heat release is that of the reaction:

$$Zr + H_2O = Zr(O) + H_2 \tag{8}$$

The partial molar enthalpy of solution of oxygen in Zr depends on the O/Zr ratio of the metal. Calorimetric data permit estimation of this quantity(9,10). For typical oxygen contents in the metal corresponding to cladding states in the zone labeled "metal" in Fig. 5, the heat of solution of oxygen is 3-5% more negative than the heat of formation of stoichiometric ZrO_2. After subtracting the heat of formation of $H_2O(g)$, the heat release from reaction(8) is 6-10% larger than that of reaction(1).

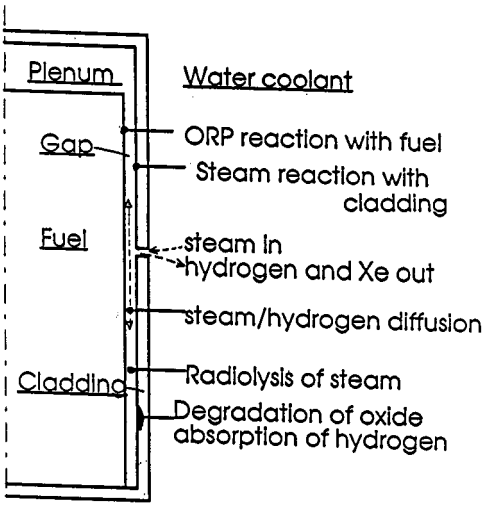

Figure. 1 Processes in a defective fuel rod

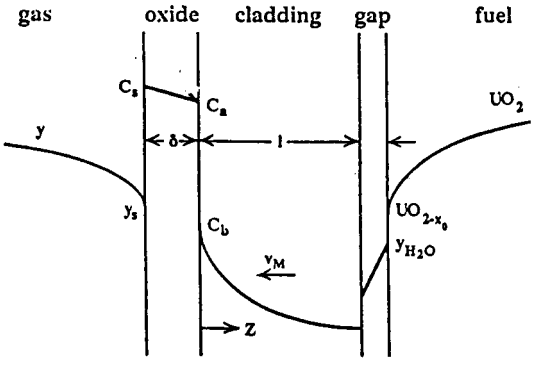

Figure 2. Radial oxygen distribution in the gas, the cladding, and the fuel during a severe fuel damage accident.

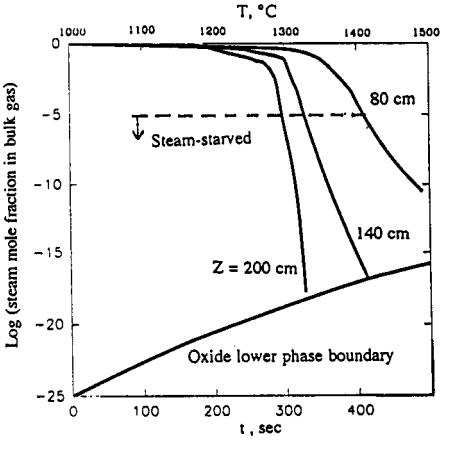

Figure. 3.

Water mole fraction in the gas as a function of time for three elevations.

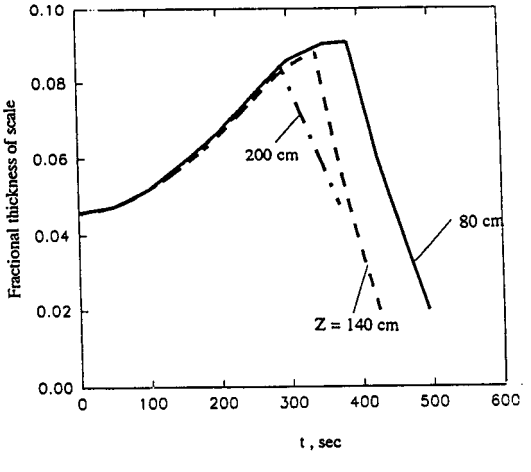

Figure. 4

Variation of fractional scale thickness with time at three elevations.

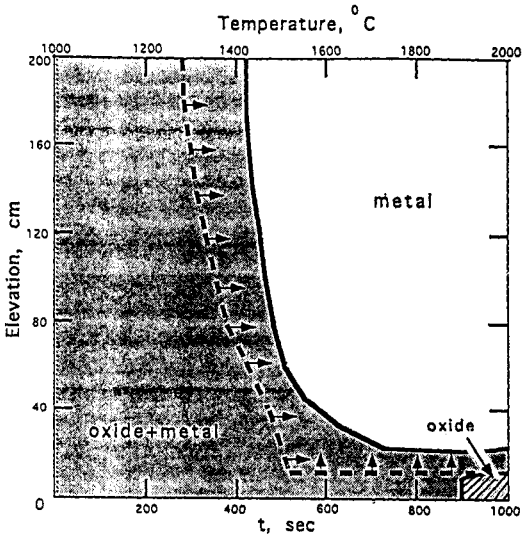

Figure. 5 Cladding state diagram

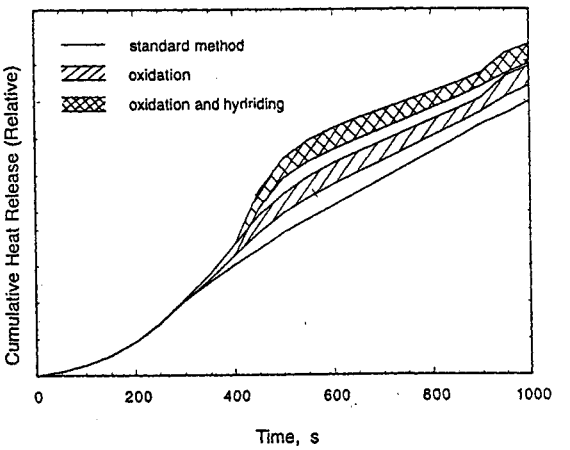

Figure. 6 Cumulative heat release due to oxidation and hydrogen absorption. The bands represent uncertainties in the solution enthalpy of oxygen in the metal.

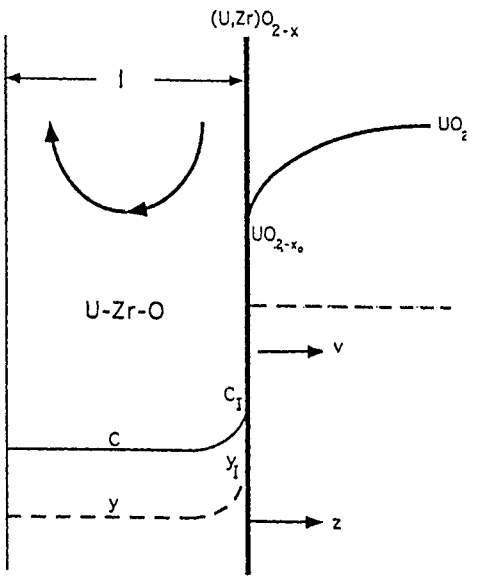

Figure. 7 Oxygen and uranium concentration distributions during fuel liquefaction

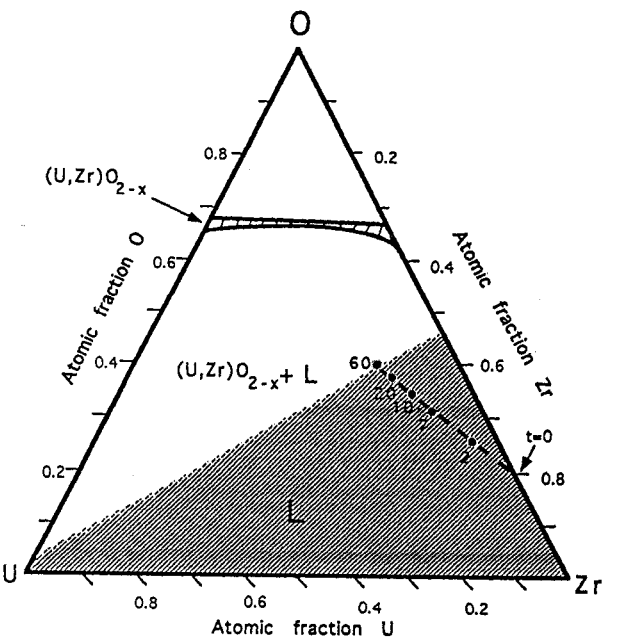

Figure 8 U-Zr-O ternary phase diagram at 2000°C. Trajectory of the melt composition during fuel liquefaction is superimposed on the diagram as the dashed line on which the numbers represent time in seconds

Regions of a core that contain Zircaloy without an oxide scale are inevitably in contact with a gas that is nearly pure H_2, which dissolves in the metal according to the reaction:

$$H_2(g) = 2H(abs) \tag{9}$$

The equilibrium of this reaction is given by Sievert's law:

$$\frac{C_H}{\sqrt{p_{H_2}}} = \exp\left(\frac{\Delta S_H}{R}\right)\exp\left(-\frac{\Delta H_H}{RT}\right) \tag{10}$$

where C_H is the H/Zr ratio of the metal in equilibrium with the gas containing H_2 at p_{H_2} atm. The thermochemical properties of hydrogen dissolution in Zircaloy are ΔH_H=-15 kcal/mole ΔS_H=-13 cal/mole-K(11). Hydrogen dissolution is not considered in current SFD modeling, but the above data show that the solubility is significant at temperatures as high as 2000°C. The principal consequences of hydrogen retention by the metal are two: First, the unoxidized metal acts as a sink of hydrogen and can alter the timing of hydrogen release during the accident. Hydrogen absorbed in the metal in the steam-starved regions is released on subsequent oxidation, because of the low solubility of hydrogen in zirconia. Second, hydrogen absorption by zirconium releases heat. While not as exothermic as the steam oxidation reaction, hydrogen uptake can significantly augment chemical heating due to oxidation. The heating effect is the sum of the product of the hydrogen content of the metal and the enthalpy of solution of hydrogen over all axial nodes. Figure 6 shows three calculations of the cumulative heat release from a fuel rod as a function of time for the transient that produced the cladding state diagram of Fig. 5. The lowest curve is the heat release based on the total amount of oxygen absorbed and assuming that the heat released per mole is the standard enthalpy of reaction(1). The next two curves are drawn as bands rather than lines to reflect the uncertainties in the partial molar heats of solution of oxygen in zirconium. The middle band includes the effect of oxygen absorption in metallic Zr, but does not consider hydrogen absorption . For the purpose of illustrating the effect of hydrogen absorption on the heat release, the upper band in Fig. 6 shows a significant increment of heat release due to dissolution of 10% of the corrosion-product hydrogen by the portions of the cladding without an oxide scale. A more detailed analysis of hydrogen-absorption heating is presented in Ref. 12 shows that the effects can be even larger than that shown in Fig. 6. The standard method for estimating heat release is valid during the early stages of the transient because the principal oxidation product is ZrO_2 and the oxide scale has not appreciably dissolved in the metal so that no hydrogen is absorbed in this time period.

Fuel Dissolution by Molten Cladding

In hydrogen-rich regions of the core, the outer oxide scale is not present on the cladding, which is all-metal with oxygen in solid solution. On melting of the cladding, the liquid metal contacts the solid fuel and dissolution of the latter begins. In addition to receiving additional oxygen, uranium from the fuel dissolves in the liquid metal forming a U-Zr-O melt. Dissolution continues until the melt is saturated in both oxygen and uranium. Analysis of this process is based on the following model: i) the only process occurring in the fuel is oxygen diffusion from the interior to the surface to supply that transported to the liquid metal; ii) the surface of the fuel is covered by a very thin layer of the solid oxide $(U,Zr)O_{2-x}$, which is in chemical equilibrium with the U-Zr-O melt at the interface. Penetration of Zr in to the bulk UO_2 is negligible because of the small cation diffusion coefficient in the solid. Since the $(U,Zr)O_{2-x}$ is very thin, it offers no resistance to element transport and its exact composition is not needed; iii) Transport of oxygen and uranium from the interface to the bulk melt takes place by natural convection mass transfer, which is driven by the higher density of the U-rich liquid at the interface compared to the Zr-rich bulk liquid. Due to the vertical configuration of the molten layer, natural convective mass transfer dominates molecular diffusion(13).

Figure 7 shows the oxygen and uranium concentration profiles during the fuel dissolution process. C is the oxygen-to-metal ratio of the melt and y is the uranium mole fraction on an oxygen-free basis. The subscript I denotes concentrations at the interface, where chemical equilibrium is assumed. As a result, C_I and y_I lie along the liquidus curve in the ternary phase shown in Fig. 8(the liquidus is the upper boundary of the shaded area in the figure). Balances on the elements U, Zr, and O are written for the melt, assuming uranium and oxygen transport from the surface to the bulk liquid by natural convection mass transfer. Oxygen transport in the fuel is described by Fick's law with allowance for the receding surface. The solution of this problem gives the temporal evolution of the melt composition(y and C) and the O/U ratio at the fuel surface. Details of the analysis are given in Ref. 14.

The dashed curve in Fig. 8 shows the computed trajectory of the composition of the bulk melt at various times during the dissolution process. The bulk composition reaches the saturation value(on the liquidus line) in less than one minute. When the liquid becomes saturated simultaneously in O and U, ~20% of the initial fuel radius has dissolved.

Conclusions

The diffusion theory analysis of Zircaloy corrosion during a severe fuel damage accident couples the kinetics of steam transport by axial convection in the coolant channel, radial transport of steam in the gas boundary layer adjacent to the cladding surface, and solid state diffusion into the cladding, which may consist of an oxide scale and a substrate metal or pure metal containing dissolved oxygen. The method provides a more accurate description of the morphological state of the cladding during such a transient than can be obtained using parabolic scaling theory. In particular, the present method allows for disappearance of the outer ZrO_2 seale on the cladding in steam-starved gas conditions.

The presence of bare cladding permits substantial quantities of hydrogen to dissolve in the metal, which affects the timing and quantity of H_2 release from the core during the accident and augments the chemical heat release from oxidation.

The ternary transport model, when coupled to the ternary phase diagram of the U-Zr-O system, provides a quantitative description of the extent of fuel dissolution by the molten cladding following contact of the liquid metal with the fuel.

References

1. T. J. Haste, *A Review of Axial Gas Communication in Oxide Fuel Rods*, NRL Springfields Report DCO 7859, UKAEA(1988)
2. K. H. Park and D. R. Olander, J. Amer. Ceramic Soc., 74, 72 (1991)
3. T. J. Heames et al, *VICTORIA, A Mechanistic Model of Radionuclide Behavior in the Reactor Coolant system under Severe Accident Conditions*, NUREG CR-5545, Rev. 1 (1992)
4. C. M. Allison et al, *Capabilities of the Integrated SCDAP/RELAP5/TRAP-MELT Severe Accident Computer Code*, Internat. Symp. on Source Term Evaluation for Accident Conditions, Columbus, Ohio(1985)
5. FAUSKE and Associates, *MAAP3.0B Computer code Manual*, EPRI report NE-7071-CCMS (1990)
6. W. Wang and D. R. Olander, J. Amer. Ceramic Soc., 76, 1242(1993)
7. D. R. Olander, *Materials Chemistry and Transport Modeling for Severe Accident Analyses in Light-Water Reactor, I - External Cladding Oxidation*, Nucl. Engin. and Design, to be published
8. D. A. Petti, Z. R. Martinson, R. R. Hobbins, and D. J. Osetek, *Results from the PBF Severe Fuel Damage Test 4-1*, Nucl. Technol., 94, 313 (1991)
9. G.Boureau and P. Gerdanian, Canadian Metall. quart., 13, 339 (1974)
10. G. Boureau and P. Gerdanian, J. Phys. Chem. Solids, 45, 141 (1984)
11. M. Moalem and D. R. Olander, J. Nucl. Mater., 178, 61 (1991)
12. D. R. Olander, *Materials Chemistry and Transport Modeling for Severe Accident Analyses in Light-Water Reactors, II - Gap Processes and Heat Release*, Nucl. Engin. and Design, to be published
13. K. T. Kim and D. R. Olander, J. Nucl. Mater., 154, 102 (1988)
14. D. R. Olander, *Materials Chemistry and Transport Modeling for Severe Accident Analyses in Light-Water Reactor, III - Fuel Dissolution*, Nucl. Engin. and Design, to be published